An optimal control approach to determine resistance-type boundary conditions from in-vivo data for cardiovascular simulations

SAE International™

Energy Consumption in ICE Lubricating Gear Pumps

2010-01-2146
Published
10/25/2010

Massimo Rundo
Politecnico di Torino

ABSTRACT

Scope of this work is the analysis of the energy consumed by lubricating gear pumps for automotive applications during a driving cycle. This paper presents the lumped parameter simulation model of gerotor lubricating pumps and the comparison between numerical outcomes and experimental results. The model evaluates the power required to drive the pump and the cumulative energy consumed in the driving cycle. The influence of temperature variations on leakage flows, viscous friction torque and lubricating circuit permeability is taken into account. The simulation model has been validated by means of a test rig for hydraulic pumps able to reproduce the typical speed, temperature and load profiles during a NEDC driving cycle. Experimental tests, performed on a crankshaft mounted pump for diesel engines, have confirmed a good matching with the simulation model predictions in terms of instantaneous quantities and overall energy consumption. The study allowed a proper screening of the power waste due to the pressure relief valve, the friction torque and the leakage losses during different stages of the engine warm-up. The outcomes from the simulation have brought to evidence that the main contribution to the consumed energy is due to the viscous friction torque, above all during the first urban cycle. Moreover, the influence of some parameters, such as the pressure setting of the relief valve and the temperature rate has been analyzed. Finally the model has been applied to an off-axis mounted gerotor pump with smaller gears diameters to quantify the improvement in power saving due to the reduction of viscous friction.

INTRODUCTION

The improvement of the engine lubricating system is becoming of great relevance due to the increasing attention on fuel consumption. Different innovations aim at reducing the power required by the lubricating pump: the improvement of the mechanical efficiency, the selection of the optimal displacement in order to match as closely as possible the minimum engine requirement, the use of variable displacement units or the closed loop control of the circuit pressure. Regardless of the adopted solution, any modification of an existing component entails unavoidable issues of reliability, space and above all cost. Therefore a detailed analysis of the consumed power in real operating conditions is necessary, to identify areas where greater potential exists for power saving. It is known that friction represents a not negligible contribution to the effective pump torque. In references [1] and [2] new rotors geometries were proposed for improving mechanical efficiency. Authors claimed a relevant reduction of friction losses, but it is not clear in what operating condition such improvement was obtained. In other studies the assessment of the energy saving attainable with new types of pumps, such as variable displacement or discrete flow units, was performed by measuring the power consumed by the component [3], [4] or the engine FMEP [5] as function of speed at constant temperature. However, it is more realistic to use as screening factor the energy absorbed by the pump to complete a standardized driving cycle. In this paper the energy analysis of a gerotor pump during a NEDC cycle, grounded on a detailed mathematical model, is presented. Simulations have been performed in the same operating conditions encountered by the pump during the cycle, in terms of speed, oil temperature and delivery pressure. Finally the experimental validation has been performed on a hydraulic test rig able to replicate with good accuracy such operating conditions [6].

SIMULATION MODEL

MESHING GEARS

In Fig. 1 a typical fixed displacement crankshaft mounted lubricating pump is presented. A couple of gears, mated so that each tooth of the outer gear is always in contact with a

tooth of the inner, form sealed chambers of fluid with variable volume. A single stage pressure relief valve discharges the excess flow to the inlet side.

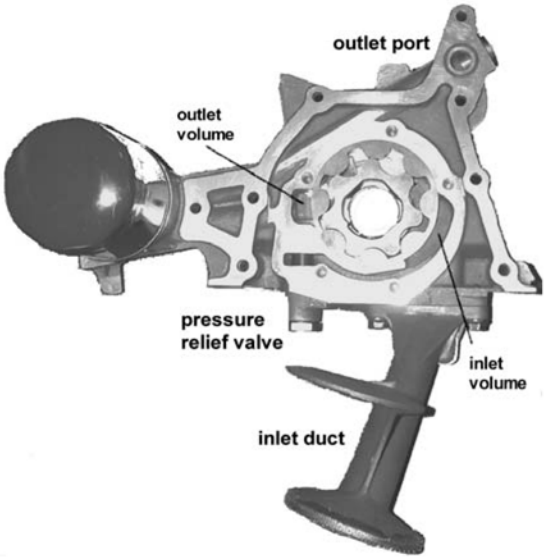

Fig. 1. crankshaft mounted pump

The pump is divided into control volumes through which fluid flows; each volume is treated as a steady-flow open thermodynamic system. Pressure variation in each chamber induced by net flow rate and angle dependent volume variation is expressed by Eq. (1):

$$\frac{dp_c}{dt} = \frac{\beta}{V_c}\left(\sum Q_i - \omega\frac{dV_c}{d\varphi}\right) \tag{1}$$

Incoming and outgoing flow rates in control volumes are evaluated with Eq. (2):

$$Q_i = C_e A_c \sqrt{\frac{2\Delta p}{\rho}} \tag{2}$$

Instantaneous values of volumes V_c and volumes derivatives of each chamber are evaluated analytically starting from the geometrical parameters of the gears [7]. Inlet and outlet flow passage areas A_c are calculated by interpolation of values stored in a data file generated by a pre-processing numerical procedure. It evaluates, for different angular positions, the passage area of the fluid as the intersection of the two surfaces limited by the profile of a chamber and the shape of the port plate (Fig. 2).

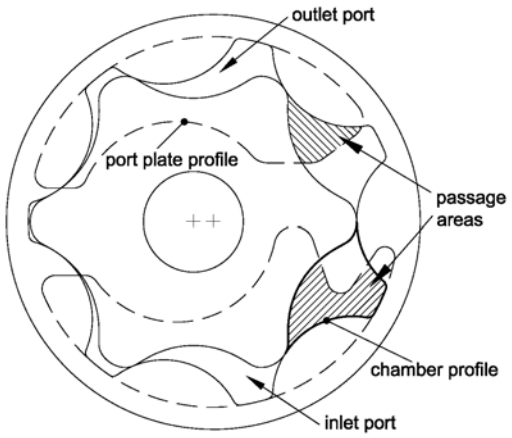

Fig. 2. flow passage areas

The following leakage flows are considered:

• between a chamber and the adjacent across teeth tips;

• across the axial clearance between gears faces and cover;

• between outlet and inlet volumes across the radial gap between the outer gear and the casing;

• to the sump across the axial gap between the inner gear and the cover (external leakage).

For each passageway, the equation expressing the flow rate through the gap valid for laminar regime is applied. The length and width of each gap is evaluated starting from the geometrical parameters of the pump. The leakage flow model is presented in greater detail in reference [8]. Pump clearances are maintained constant during the simulation, except for the external leakage. In fact in crankshaft mounted pumps, the cover plate deformation due to the delivery pressure generates a not negligible increment of the axial gap [9] as also testified by experimental results presented hereafter. Thus the leakage flow to the sump is evaluated with Eq. (3):

$$Q_L = \frac{b(h_0 + k \bullet p_d)^3}{12\mu L} \bullet p_d \tag{3}$$

being h_0 the axial clearance corresponding to zero pressure and k an experimental coefficient. Moreover the pressure drops through the inlet pipe and the outlet duct (from the internal delivery volume to the outlet port) are also considered.

FRICTION TORQUE

The absorbed torque is evaluated as the sum of two terms: the indicated torque M_h and the friction torque M_f. The former is calculated starting from the simulated indicated cycle as the

summation of products between the volume derivative of each chamber V_c and its pressure p_c evaluated by Eq. (1):

$$M_h = \sum_{i=1}^{N} -\frac{dV_c}{d\varphi} \bullet p_c \qquad (4)$$

whereas the latter is evaluated by interpolation of a data table obtained by experimental tests at different values of delivery pressure, speed and temperature. The term M_h differs from the theoretical torque M_{th} due to the fluid friction loss through hydraulic resistances inside the pump, such as inlet and outlet ports, suction and delivery ducts. The friction torque M_f can be subdivided in two terms [10]: a torque depending proportionally on speed M_μ generated by viscous friction between sliding surfaces and the torque loss M_p, depending proportionally on delivery pressure, necessary to overcome friction between surfaces in direct contact, where boundary lubrication regime occur. The term M_μ is evaluated by extrapolation to zero pressure of the total measured friction torque, for each value of speed and temperature, while the pressure dependent term M_p is obtained as the difference between total friction and viscous torques.

POWER AND ENERGY EVALUATION

The consumed power can be subdivided in six terms evaluated as follows:

• the useful power P_u is the product between the flow rate delivered to the circuit Q_u and the pressure at pump outlet p_u;

• the power lost in the relief valve P_{RV} is the product between the flow rate discharged by the valve and its upstream pressure (i.e. in the internal delivery volume p_d);

• the viscous friction power loss is the product between viscous torque M_μ and speed;

• the boundary friction power loss is the product between torque M_p and speed;

• the hydraulic power loss P_h, that takes into account the internal pressure drops, is given by Eq. (5):

$$P_h = (M_h - M_{th})\omega \qquad (5)$$

• the leakage power loss P_L is calculated from Eq. (6):

$$P_L = M_{th}\omega - P_u - P_{RV} \qquad (6)$$

The consumed energy during the driving cycle is calculated by integration of the corresponding power.

PUMP LOAD

The characteristic equation of the lubrication circuit expressing the flow rate Q_u as function of the pump outlet pressure p_u can be well approximated with Eq. (7):

$$Q_u = a(T) \cdot p_u^{b(T)} + c(T,\omega) \qquad (7)$$

where coefficients $a(T)$, $b(T)$ and $c(T,\omega)$ are functions of temperature and speed. They are determined starting from experimental data collected on the engine [6]. Equation (7) also accounts for the pressure drop in the fluid conditioning unit (filter and heat exchanger) and reproduces the outlet pressure of the pump measured on the engine with an error of ± 0.2 bar at equal flow rate.

MODEL IMPLEMENTATION

Figure 3 shows the simulation model in the AMESim™ environment [11] used for evaluating the energy consumed during the driving cycle. The meshing gears are simulated by a "supercomponent" made up of elements belonging to a proprietary library [12]; it includes variable volume chambers, inlet and outlet ports and leakage passageways. This component receives as input the speed profile, supplied by a data file, and calculates the indicated torque M_h. Another supercomponent, created with the Hydraulic Component Design Library, simulates the pressure relief valve.

The flow rate required by the lubricating circuit is calculated by an element implementing Eq. (7). Viscous and boundary friction torques are obtained by linear interpolation of data tables as function of pressure, speed and temperature. The temperature versus time is read from a data file and supplied to several components: lubricating circuit, friction elements and gears, for taking into account the variation of the leakage flow as the temperature increases. Fluid density is considered constant, since it was checked that this approximation has a negligible influence on the energy calculation (less than 1 kJ throughout the whole NEDC). To reduce the CPU time and the size of the results file, the time scale is divided by a factor 100 and consequently the calculated powers are multiplied by the same factor.

TEST RIG

LAYOUT

In Fig. 4 the hydraulic scheme of the test rig used for model validation is shown; main components are:

• M1: variable speed electric drive.

• TF: torque meter HBM T10F, with range 0÷50 Nm and precision class 0.1.

• R1: electro-pneumatic actuated proportional flow control valve.

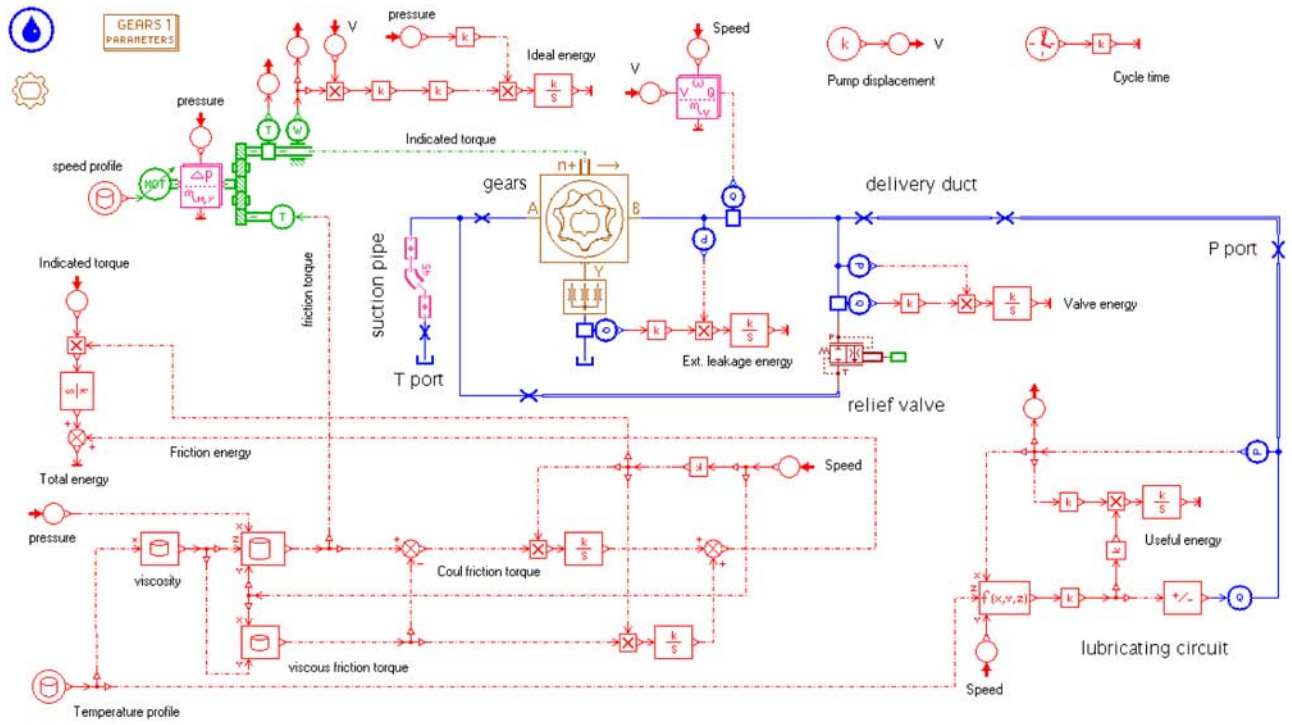

Fig. 3. simulation model layout

• P1: pressure transducer GS XPM5, with range 0÷20 bar and linearity error ± 0.25% F.S.

• FM: mass flow meter MICROMOTION CMF100M.

• T1, T2, T3, T4: PT100 thermo-resistances.

• EH: 10 kW electric heating element.

• SC: oil cooler composed by a water-oil heat exchanger and a chiller.

The unit under test is a 15.3 cc/rev crankshaft mounted pump for Diesel engines with direct pilot pressure relief valve and setting of 6.5 bar. Tank temperature is obtained from the average of readings of differently located thermo-resistances T1 and T2. Torque measured by the torque-meter is reduced by the quota relative to the bearings of the interface block: this contribution is evaluated through an expression derived from experimental measurements without the pump and at varying speed being temperature given from T4. The rig utilizes synthetic base oil with SAE grade 5W30.

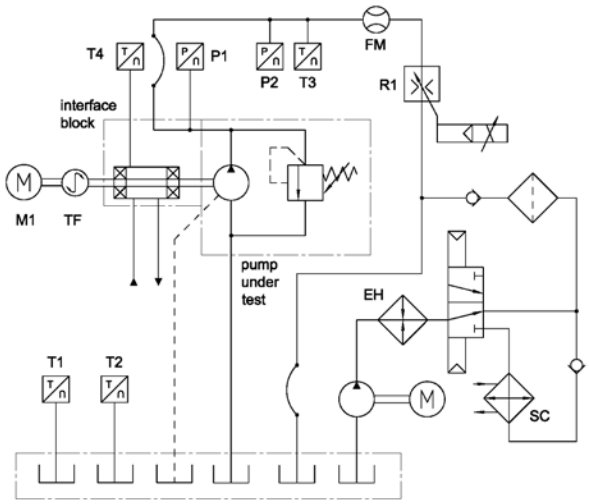

Fig. 4. simplified layout of the hydraulic circuit

OPERATING MODES

The load on the pump is generated by the valve R1 that can be controlled in either open or closed loop, while the feedback signal can be supplied by a rig transducer or can be a function of different signals. In particular to replicate the curves expressed by Eq. (7), a closed loop control is implemented so that valve R1 originates a flow passage that reproduces, for each temperature and velocity condition, the resistance generated by the lubrication circuit. The engine velocity profile during the driving cycle can be assigned as

set point for the electric motor M1. Inlet or outlet pump temperature can be controlled in a closed loop in the range 5÷140 °C acting on both the heater and the cooler. Alternatively, an experimental oil temperature profile, measured on the engine, can be reproduced acting in an open loop on the power of the electric resistance EH. The operating procedure for testing a lubricating pump during a driving cycle is reported in detail in reference [6].

PRELIMINARY TESTS

FRICTION TORQUE MAP

For the construction of the data table used for the evaluation of the friction torque, the pump was tested in steady-state conditions at six values of temperature (20-30-40-60-80-100 °C), six values of speed (from 500 to 3000 rpm with a step of 500 rpm) and with delivery pressure ranging from 1 bar to the maximum value. In Fig. 5 and Fig. 6 the total friction torque M_f is reported for two different oil temperatures. The graphs are obtained by subtracting the term M_h, evaluated in the same operating condition by the simulation model with Eq. (4), from the measured torque. It is worthwhile to notice that at low temperature the experimental data are well approximated by straight lines, except at very low speed and high pressure. On the contrary, at high temperature the linear regression can be applied only if the speed is greater than 1500 rpm, while at lower speed, as the pressure increases, the torque grows exponentially. This can be understood by referring to the Stribeck curve: in fact low viscosity, low speed and high load lead to an increment of the friction coefficient, due to the transition from hydrodynamic to mixed or boundary lubrication regime.

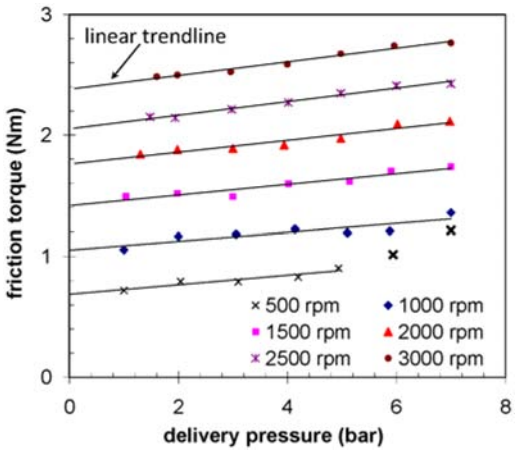

Fig. 5. total friction torque at 30 °C

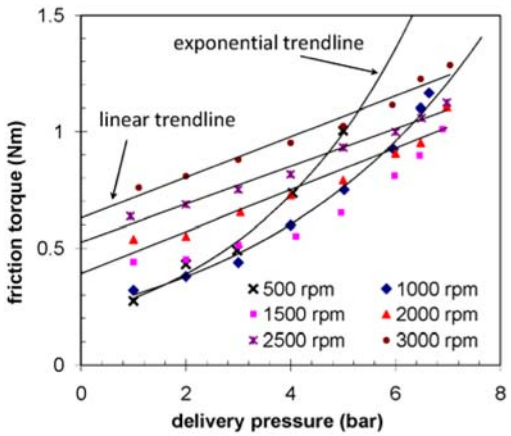

Fig. 6. total friction torque at 100 °C

The friction torque corresponding to zero pressure, extrapolated from tests performed at different temperatures and speed, is depicted in Fig. 7. It represents the viscous friction contribution.

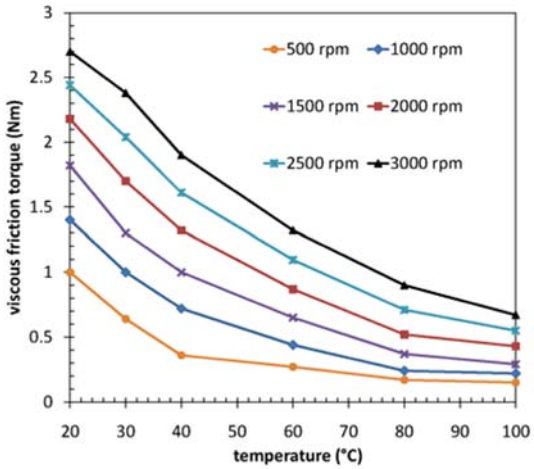

Fig. 7. viscous friction torque map

COVER PLATE DEFORMATION

The need to take into account the variation of the axial gap height due to the cover plate deformation is confirmed by the experimental measure of the leakage flow to the oil sump, reported in Fig. 8 at different pump speeds and at constant oil temperature.

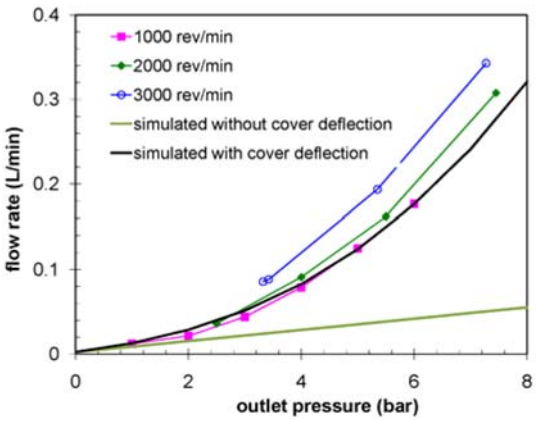

Fig. 8. external leakage flow as function of pressure

The test was executed by measuring the time required to fill a 200 cc burette with oil leaking from the pump[1]. The relationship between flow and pressure in case of laminar regime should be linear, while the measured leakage flow is nearly proportional to the square of the pressure and this behavior can only be justified by an increment of the clearance. The flow rate increase with speed at the same pressure is likely originated by the reduction of oil viscosity inside the gap, due to heat generated by viscous friction. The measurement of the cover plate deformation was performed by means of a noncontact linear proximity transducer KAMAN KD2300-1SUM (range 0-1.25 mm and resolution 0.1 µm) fitted on the test rig interface as shown in Fig. 9. The sensor measures the distance from the cover plate in correspondence of the delivery volume of the pump.

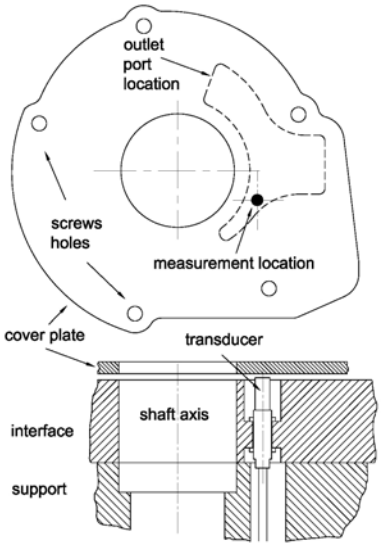

Fig. 9. location of the proximity transducer

The measure of the deformation as function of the delivery pressure is reported in Fig. 10; from this graph it is possible to appraise the value of the constant k in Eq. (3) that takes into account the increment of the axial gap (about 4 µm/bar).

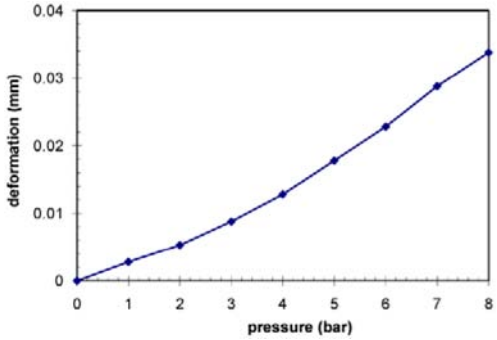

Fig. 10. deformation of the cover plate

SIMULATION OF DRIVING CYCLE

MODEL VALIDATION

The simulation model uses the same temperature profile (Fig. 11) measured on the test rig at the pump outlet by the transducer T3 during the NEDC cycle. The maximum difference with respect to the temperature sensed on the engine at equal time is 2 °C. In the same figure tank temperature is also reported.

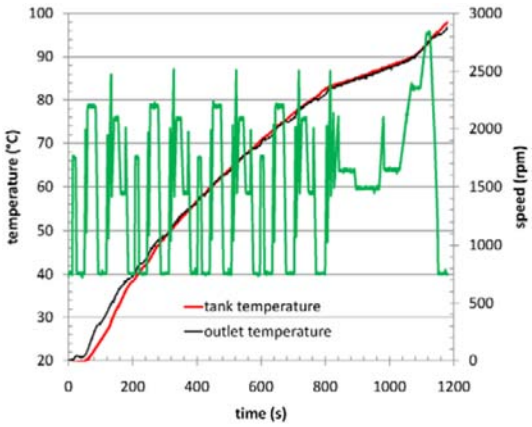

Fig. 11. temperature and speed profile measured on the test rig

The model has been validated by superimposing the simulated flow rate (Fig. 12), pressure at pump outlet (Fig. 13) and torque (Fig. 14) as function of time with the quantities measured on the test rig. The maximum error is 1 L/min for the flow rate, 0.3 bar for pressure and 0.1 Nm for torque. The measured energy required for the whole NEDC cycle amounts to 428.9 kJ, corresponding to a mean power of

[1] This test was performed on a different test rig with 15W40 motor oil at 38 °C.

363 W, while the simulated value is 435.4 kJ, with an error of 1.5%. The measured useful energy is 186 kJ, while from the simulation a value of 185.1 kJ has been obtained.

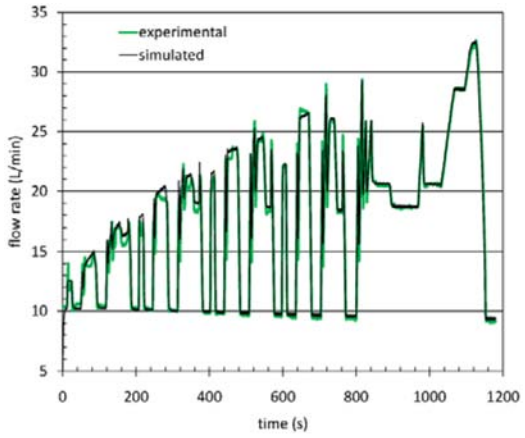

Fig. 12. flow rate during NEDC

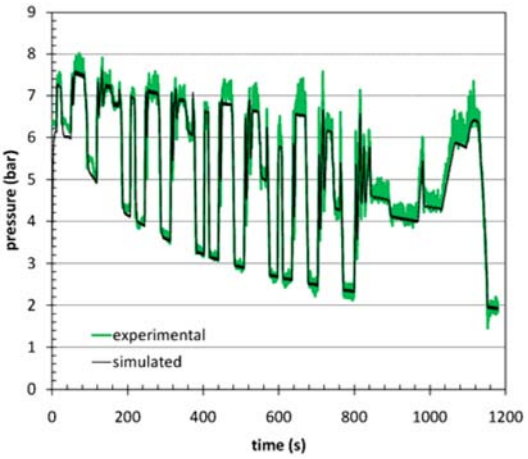

Fig. 13. pump pressure during NEDC

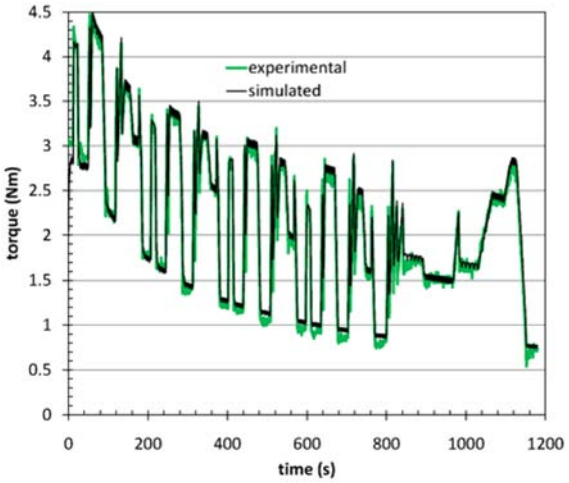

Fig. 14. pump torque during NEDC

The small differences between instantaneous experimental and simulated quantities could be due to several reasons. First of all during rapid speed variations, essentially in correspondence of gear shifts, circuit permeability could not be properly reproduced. To partially overcome this drawback a variable closed loop gain for controlling the valve E2 has been used: a low value during constant speed periods, while a higher value during speed slopes. Secondly, it must be considered that the data file used for evaluating the friction torque has been obtained in thermal steady-state conditions, while, on the contrary, during the cycle both speed and oil temperature vary quite quickly. Finally in the first urban cycle the pressure relief valve recirculates to the inlet volume about half of the generated flow rate, producing a faster increment of the outlet temperature with respect to tank temperature as testified in Fig. 11. Therefore on the test rig the pump will work with different temperatures at inlet and outlet side, while in the simulation model a uniform temperature, equal to the outlet value, is considered. However a difference of 6.5 kJ after 1180 s corresponds to an error of 5.5 W on the mean power and just 0.035 Nm on the torque, being 1503 rpm the mean cycle speed.

ENERGY ANALYSIS

Figure 15 shows the cumulative energies simulated during the NEDC driving cycle, while in Fig. 16 the relative percentage contribution of each loss at the end of the cycle is reported. It is evident that the viscous friction torque plays an important role, being its contribution about 29% of the total consumption. The energy associated to the viscous torque grows very rapidly in the first part of the cycle due to the low oil viscosity, in particular at the end of the first urban cycle about 41% of the energy is consumed by viscous friction. The pressure relief valve regulates only at low temperature, therefore its contribution remains constant starting from the 3rd urban cycle. About 50% of the power associated with the leakage flow originates from axial clearance, confirming the importance of the cover plate deformation.

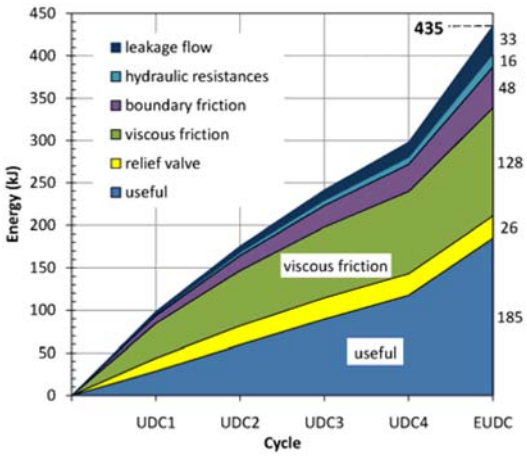

Fig. 15. cumulative energy with crankshaft mounted pump

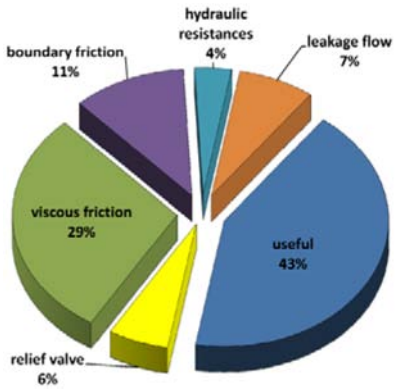

Fig. 16. percent contribution of consumed energy

It is worth to notice that a not negligible fraction of the useful energy is dissipated in the oil conditioning unit, i.e. filter and heat exchanger. However this quota cannot be ascribed to the pump, but rather to circuit losses. The remaining part of the energy available in the circuit main gallery is also completely dissipated, since the lubricating network is exclusively made up of resistive components (bearings, piston cooling jets, distributed resistances, etc.). Therefore, the whole mechanical energy required by the pump (435 kJ) is transformed into heat, which is transferred to the oil and contributes to its temperature increase. The thermal energy E_t necessary to heat the oil contained in the sump from the initial value of 20°C to the value reached at the end of the driving cycle can be evaluated starting from the temperature profile:

$$E_t = V_{oil} \int_{t1}^{t2} c_p(T)\rho(T)\dot{T}dt \qquad (8)$$

Assuming a total oil volume of 6 liters, from Eq. (8) a value of 870 kJ is obtained. This energy represents only a fraction of the heat received by the oil, since the remaining part is transferred through the circuit walls, the oil sump, the bearings surfaces and the filter. If, to a first approximation, during the warm-up oil retained 40% of the received heat [13], the heat energy for increasing fluid temperature up to 97 °C would be 2.2 MJ. Thus the contribution to oil heating due to pump losses and pressure drops throughout the circuit can be appraised to be of about 20%.

SENSITIVITY ANALYSIS

INFLUENCE OF TEMPERATURE RATE

In the last 20 years the oil temperature rate in modern engines has remained substantially unchanged [14]. This is also confirmed by data collected from the open literature (Fig. 17), where the maximum range of variation of the temperature for very different engines can be estimated to be of about 15-20 °C at equal time. In particular profile A refers to an experimental measurement on a midsize gasoline engine with cold start at 25 °C [15], curve B was measured on a 2.4 L diesel engine [16], curve C is simulated for a V8 gasoline engine [17], curve D is simulated [18] and eventually profile E has been simulated in the AMESim environment by means of the demo Vehicle Thermal Management [11]. To assess the influence of the temperature variation on calculated energy, two new profiles have been constructed by interpolation of the curves found in the literature. The upper profile, representing the higher temperature rate, is quite similar in the first urban cycle to the reference curve used for the previous simulation, while it differs of about 15 °C in the extra-urban cycle. Instead the lower profile differs of about 10 °C at low temperature with respect to the reference curve, while the difference is lower at higher temperature.

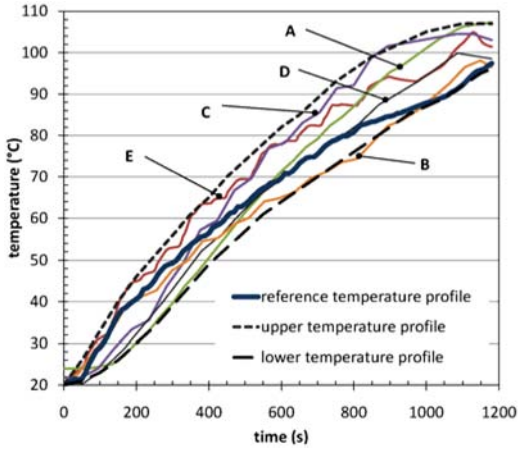

Fig. 17. various temperature profiles during NEDC

The simulation of the driving cycle has been repeated with these extreme profiles: the results are reported in Fig. 18.

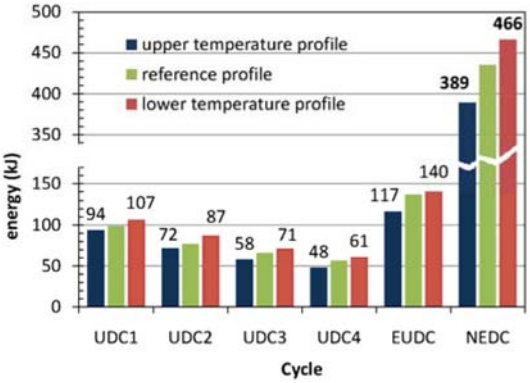

Fig. 18. influence of temperature profile

It can be noticed that in the first UDC, a temperature difference of 16 °C between the upper and lower profiles at the end of the cycle (at 195 s), with equal starting temperature of 20 °C, generates an energy variation of 13 kJ (94 kJ against 107 kJ). The same difference of 13 kJ (48 kJ versus 61 kJ) is observed in the 4th urban cycle, even if in this case temperature profiles differ of 17°C at the beginning (at 585 s) and 20°C at the end (at 780 s) of the cycle. The reason is the non-linear relationship between oil viscosity and temperature, therefore the viscosity is reduced by 51% for the first 15 °C of heating and only by 31 % from 70°C to 85 °C. With respect to the reference profile, the reduction of total energy with the upper curve is 46 kJ, corresponding to a decrease of 10%, while using the lower profile an increment of 7% (31 kJ) is obtained.

INFLUENCE OF THE PRESSURE SETTING OF THE VALVE

The actual trend for lowering consumed power is the reduction of pressure in the circuit. In Fig. 19 the energies simulated with different values of pressure setting of the valve are shown. They have been obtained by reducing the preload of the valve spring.

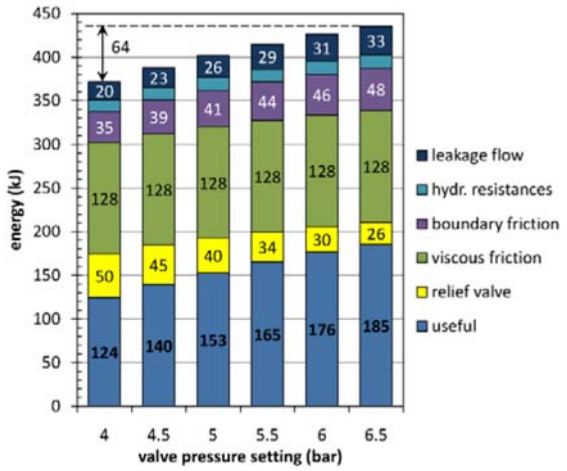

Fig. 19. influence of valve pressure setting

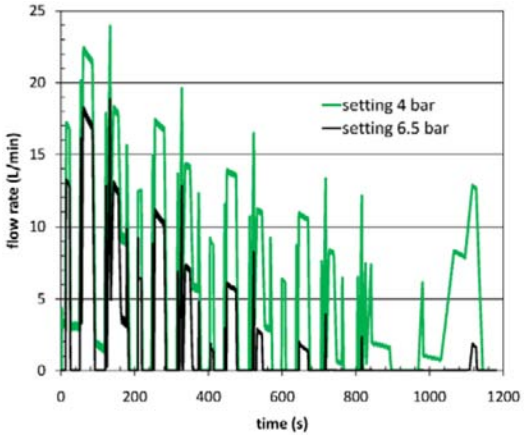

Fig. 20. flow rate through the relief valve

The lowering of 40% of the valve setting generates a decrease of 64 kJ of consumed energy, corresponding to about 15%. The reduction of pressure decreases useful power, not only because the circuit is pressurized at a lower value, but also because the received flow rate is reduced, since the circuit is constituted by resistive components. This reduction is distributed quite uniformly among the cycles. A lower pressure setting entails an increment of the energy loss in the valve, in fact, despite a lower pressure drop, the discharged flow is higher since the valve operates more frequently. In Fig. 20 the simulated flow rate through the relief valve with two different pressure ratings is reported: at 6.5 bar the valve is open for 26% of time, while at 4 bar for 66%. However the increment of the power wasted by the valve is counterbalanced by the decrease of boundary friction torque and leakage flow, both functions of pressure, therefore on the whole the total consumed energy is reduced.

This entails a decrease of heat transferred to the oil and consequently a lowering of the temperature rate. Nevertheless, since for increasing oil temperature from 20 °C to 97 °C about 2.2 MJ are necessary, it is possible to estimate that a decrease of 64 kJ will induce a reduction of the final temperature of about 2÷3 °C. Therefore the use in the simulation model of the same temperature profile for different values of the valve setting will generate a negligible error.

INFLUENCE OF CIRCUIT PERMEABILITY

Pump displacement should be so selected to match as closely as possible the flow rate required by the circuit, so that an optimal pressure level in the main gallery can be reached. Nevertheless it is possible that the same pump might be mounted on various types of engines with different flow-pressure characteristics. Moreover, even on the same engine, circuit permeability increases as bearing clearances grow. In Fig. 21 the energy as function of the percentage variation of circuit permeability with respect to the reference flow-pressure curve is reported. The simulation has been performed by applying a constant gain to the flow rate expressed by Eq. (7). The increment of circuit permeability yields the reduction of the delivery pressure and consequently the decrease of the Boundary friction torque and the leakage flow. In the pressure relief valve the reduction of the power loss is more evident since it is also due to the decrease of the discharged flow. The variation of the useful energy is quite negligible, in fact the reduction of delivery pressure is counterbalanced by the increment of flow rate delivered to the circuit. The total energy decreases almost proportionally with the increment of the circuit permeability; in particular a variation of ±20% in circuit permeability generates a deviation of ±7% in the consumed energy.

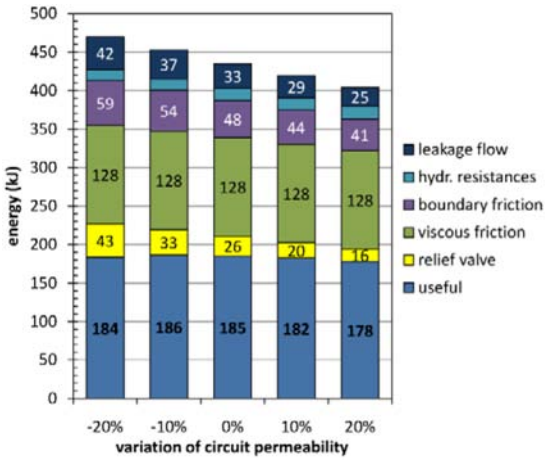

Fig. 21. influence of circuit permeability

SIMULATION OF OFF-AXIS MOUNTED PUMP

Off-axis mounted pumps allow a reduction of the viscous friction, due to a lower ratio between the diameter and the width of the gears [1]. In this way, at equal displacement, the peripheral velocity of the rotors can be reduced. Another advantage is the possibility to vary the transmission ratio between engine and pump, in order to obtain a reduction of the rotary speed and therefore a further decrease of the surfaces sliding velocity; however in this case it is necessary to increment the axial width for increasing the theoretical flow rate. To evaluate the advantage of this solution with respect to a direct drive, a 19.8 cc/rev off-axis mounted pump has been simulated in the same circuit. The ratio between external diameter of the outer gear and its axial width is 2.5, while in the directly driven pump this value is 7.3. To assess the influence of gears geometry, in the simulation model the same valve and ducts of the crankshaft mounted pump have been used. Moreover for obtaining the same flow rate delivered to the circuit, a transmission ratio of 0.695 has been set, even if the ratio between pumps displacements is 0.773. In fact, the volumetric efficiency of the off-axis pump used for the test is higher due to smaller tooth tip clearances and negligible external leakage. The decrease of pump speed along with smaller gears diameters reduces the peripheral velocity of the outer rotor by 46%. Figure 22 shows the pump mounted on the test rig for the measurement of friction torque to be supplied to the simulation model[2]. Transducer P1 senses the pressure in the internal delivery volume of the pump.

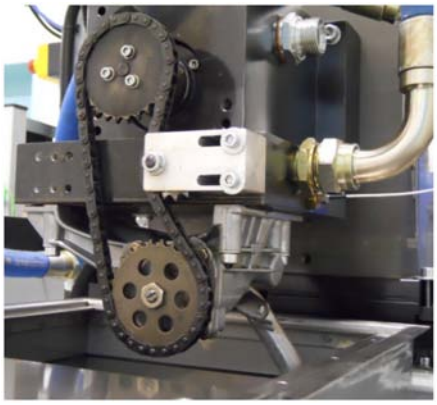

Fig. 22. off-axis pump mounted on the test rig

In Fig. 23 the energies cumulated during the cycle are shown, while in Fig. 24 the percentage contribution at the end of the EUDC is reported. The mechanical energy consumed by the pump is 287 kJ, which represents 66% of the value required by the crankshaft mounted pump at equal useful energy. Most of the difference is due to the remarkable reduction of viscous friction. However the drawback of the off-axis mounted solution is the increment of the axial width and the higher cost due to a greater number of components.

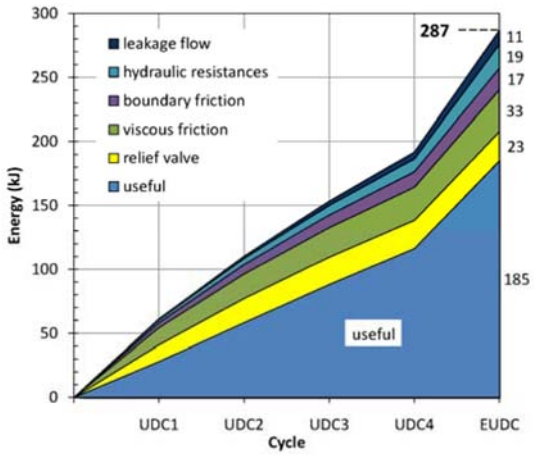

[2]For these tests the pump has been driven with a transmission ratio 1:1

Fig. 23. cumulative energy with off-axis mounted pump

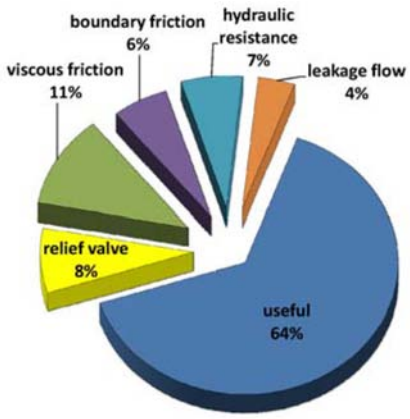

Fig. 24. percent contribution of consumed energy

In Fig. 25 the crankshaft mounted pump is contrasted with the off-axis pump in terms of overall efficiency, defined as the ratio between the mean useful power and the mean expended power. In both cases the higher efficiency is obtained in the 4th urban cycle and in the extra-urban cycle due to the lower oil viscosity and to the higher circuit permeability. In fact in this operating condition viscous friction is significantly lower and the intervention of the pressure relief valve is sensibly reduced.

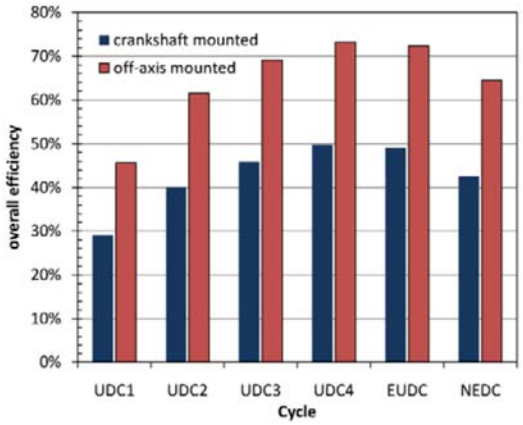

Fig. 25. overall efficiencies

CONCLUSIONS

This study allowed to discern the percentage contribution of different power losses in both crankshaft and off-axis mounted gerotor lubricating pumps. The analysis has been performed in the same operating conditions encountered during the driving cycle, in terms of temperature, speed and load. Simulations have been repeated with different values of temperature rate, valve setting and circuit permeability, in order to generalize as much as possible the results obtained on the reference lubricating circuit. The study brings to evidence that friction plays a primary role in crankshaft mounted pumps, being its contribution about a third of the overall energy consumed during a NEDC cycle. Moreover in the first UDC cycle more than 50% of the energy is lost in friction due to the high oil viscosity. In off-axis mounted pumps the influence of viscous friction is remarkably reduced, due to the lower peripheral velocity of the external rotor. This leads to a considerable increment of the mean overall efficiency of the pump in every stage of the driving cycle. Nevertheless, even with this kind of pump, in the first urban cycle the efficiency is lower than 50%. The loss in the pressure relief valve has a range from 5% to 13% of the total energy, depending on temperature profiles, engine permeability and pressure setting. Thus, the removal of the pressure relief valve and the substitution of the fixed displacement pump with a variable displacement unit could lead to unsatisfactory results, unless a reduction of friction is also obtained.

REFERENCES

1. Haas, A., Esch, T., Fahl, E., Kreuter, P. et al., "Optimized Design of the Lubrication System of Modern Combustion Engines," SAE Technical Paper 912407, 1991, doi: 10.4271/912407.

2. Fujiwara, S., "High Efficiency Oil Pump Rotor With New Tooth Profile," SAE Technical Paper 2004-01-0498, 2004, doi:10.4271/2004-01-0498.

3. Neukirchner, H., Kramer, M., and Ohnesorge, T., "The Controlled Vane-Type Oil Pump for Oil Supply on Demand for Passenger Car Engines," SAE Technical Paper 2002-01-1319, 2002, doi:10.4271/2002-01-1319.

4. Toyoda, F., Kobayashi, Y., Miura, Y., and Koga, Y., "Development of Variable Discharge Oil Pump," SAE Technical Paper 2008-01-0087, 2008, doi: 10.4271/2008-01-0087.

5. Koch, F., Maassen, F., and Geiger, U., "Development of Modern Engine Lubrication Systems", SAE Technical Paper 970922, 1997, doi:10.4271/970922.

6. Rundo, M. and Squarcini, R., "Experimental Procedure for Measuring the Energy Consumption of IC Engine Lubricating Pumps during a NEDC Driving Cycle," *SAE Int. J. Engines* **2**(1):1690-1700, 2009, doi:10.4271/2009-01-1919.

7. Fabiani, M., Mancò, S., Nervegna, N., Rundo, M. et al., "Modelling and Simulation of Gerotor Gearing in Lubricating Oil Pumps," *SAE Transactions, Journal of Engines* **108**(3): 989-1003, 1999.

8. Mancò, S., Nervegna, N., Rundo, M. et al., "Gerotor Lubricating Oil Pump for IC Engines," *SAE Transactions, Journal of Engines* **107**(3): 2267-2284, 1998, doi: 10.4271/982689.

9. Kini, S., Mapara, N., Thoms, R., Chang, P. et al., "Numerical Simulation of Cover Plate Deflection in the Gerotor Pump," SAE Technical Paper 2005-01-1917, 2005, doi:10.4271/2005-01-1917.

10. Ivantysyn, J, Ivantysynova, M., "Hydrostatic Pumps and Motors", Akademia Books International, New Delhi, India, ISBN 81-85522-16-2:71-72, 2001.

11. Imagine.Lab AMESim (Rev 9), LMS Imagine SA, 2009.

12. Mancò, S., Nervegna, N., Rundo, M., "A Contribution to the Design of Hydraulic Lube Pumps", *The Int. Journal of Fluid Power* **3**(1): 21-31, 2002.

13. Trapy, J.D. and Damiral, P., "An Investigation of Lubricating System Warm-Up for the Improvement of Cold Start Efficiency and Emissions of S.I. Automotive Engines," SAE Technical Paper 902089, 1990, doi:10.4271/902089.

14. Andrews, G.E., Ounzain, A.M., Li, H., Bell, M. et al., "The Use of a Water/Lube Oil Heat Exchanger and Enhanced Cooling Water Heating to Increase Water and Lube Oil Heating Rates in Passenger Cars for Reduced Fuel Consumption and CO_2 Emissions During Cold Start," SAE Technical Paper 2007-01-2067, 2007, doi: 10.4271/2007-01-2067.

15. Kunze, K., Wolff, S., Lade, I., and Tonhauser, J., "A Systematic Analysis of CO_2-Reduction by an Optimized Heat Supply during Vehicle Warm-Up," SAE Technical Paper 2006-01-1450, 2006, doi:10.4271/2006-01-1450.

16. Brace, C. J., Hawley, G., Akehurst, S., Piddock, M., Pegg, I., "Cooling system improvements - assessing the effects on emissions and fuel economy", *Proc. IMechE, Part D: J. Automobile Engineering*, **222**(4): 579-591, 2008. DOI: 10.1243/09544070JAUTO685.

CONTACT INFORMATION

Massimo Rundo
massimo.rundo@polito.it
http://www.polito.it/fluidpower

ACKNOWLEDGMENTS

The present work has been partially performed under a research contract with Pierburg Pump Technology SpA. The author acknowledges permission of publishing the present material.

DEFINITIONS/ABBREVIATIONS

A_c
: Flow passage area

b
: Gap width

C_e
: Flow coefficient

c_p
: Constant pressure specific heat

E_t
: Heat

h_0
: Gap height at zero pressure

k
: Cover plate deformation coefficient

L
: Gap length

M_f
: Total friction torque

M_h
: Indicated torque

M_p
: Pressure dependent friction torque

M_{th}
: Theoretical torque

$M\mu$
: Viscosity dependent friction torque

N
: Number of variable volume chambers

p_c
Chamber pressure

p_d
Pressure in delivery volume

p_u
Pressure at outlet port

P_h
Hydraulic power loss

P_L
Leakage power loss

P_{RV}
Power lost in the pressure relief valve

P_u
Power available at pump outlet

Q_i
Flow rate through area A_c

Q_u
Flow rate at pump outlet

T
Oil temperature

V_c
Chamber volume

V_{oil}
Total volume of oil in the circuit

β
Fluid bulk modulus

Δp
Pressure drop

μ
Fluid dynamic viscosity

ρ
Fluid density

φ
Shaft angular position

ω
Shaft angular velocity

FMEP
Friction Mean Effective Pressure

The Engineering Meetings Board has approved this paper for publication. It has successfully completed SAE's peer review process under the supervision of the session organizer. This process requires a minimum of three (3) reviews by industry experts.

ISSN 0148-7191

doi:10.4271/2010-01-2146

SAE Customer Service:
Tel: 877-606-7323 (inside USA and Canada)
Tel: 724-776-4970 (outside USA)
Fax: 724-776-0790
Email: CustomerService@sae.org
SAE Web Address: http://www.sae.org
Printed in USA